Model fermion Monte Carlo method with antithetical pairs

Zhiping Liu, Shiwei Zhang,* and M. H. Kalos
Center for Theory and Simulation in Science and Engineering and Laboratory of Atomic and Solid State Physics, Cornell University, Ithaca, New York 14853
(Received 7 February 1994)

We consider certain model systems within which we seek solutions of the Schrödinger equation that are antisymmetric on inversion in the origin. We find geometrical constructions that define sequences of correlated random walks for which the overlap with antisymmetrical test functions are asymptotically constant. The emphasis here is on problems in two dimensions, but the methods generalize to many dimensions and to certain other model problems.

PACS number(s): 02.70.−c, 05.30.−d, 03.65.Ge

I. INTRODUCTION

In attempting to understand the essence of the "sign problem" [1] for the fermion Monte Carlo (MC) method, we have formulated and studied a number of highly simplified model problems. One that has been the subject of many "thought calculations" is the solution of the Schrödinger equation in a two-dimensional box. We have sought simple elaborations of random walks that generate populations having a stable overlap with test functions that are antisymmetric on inversion in the origin. Such conceptual algorithms have always been developed with the pretense that a nodal line that will generate an exact fixed-node solution [1] is not known.

We have recently solved this problem and, in the process, a class of related problems. This paper is devoted to the exposition of the new ideas that underlie the techniques. It is important to emphasize that, while the original problem was one in which a class of nodal lines is known, that is not true for all the models for which the new constructions apply.

Our interest in highly simplified model problems such as this lies in part in their didactic interest, and in part in the hope that important basic issues can be clarified through their solutions. Perhaps the most basic issue among these is the question whether antisymmetric solutions of the Schrödinger equation necessarily require large ensembles of interacting walkers [2–4] or can be treated using independent walkers, or possibly correlated pairs (triplets, quartets,...). Our previous failure to find an elegant solution in the latter category led us to return to the use of large ensembles [4].

This paper exhibits a method in which pairs of antithetic walkers are created and sometimes destroyed at predefined surfaces. These surfaces are not, in general, nodal surfaces for the antisymmetric solution. We show that the original problem of a particle in a square box can be solved that way. We show explicit numerical solutions for a particle in a rectangular and in a parallelogram, and to a nonphysical Gaussian model introduced a few years ago [5]. We sketch how the method applies to a particle in enclosures of many shapes (that map into themselves on inversion in the origin) and when potentials that satisfy certain inequalities are introduced. Finally, we remark that the method can be carried out using pairs of walkers in the d-dimensional rectangular box.

By way of a simple introduction, we will discuss the solution of Schrödinger equation with the lowest energy that vanishes on the boundary of an arbitrary parallelogram and that has inversion antisymmetry.

The parallelogram is shown in Fig. 1 along with the longer diagonal lm (which cannot be a nodal line of the solution we seek) and with a line pq through the origin perpendicular to that diagonal. These symmetry lines divide the domain into regions A,B,C,D. Region A is divided into A1 and A2 as shown. A1 is the reflection of D in lm and also the reflection of B in pq.

Walkers are started only in domain A. These walkers follow continuous Brownian paths, or equivalently domain Green's function Monte Carlo (GFMC) [6–8] paths, and multiply along the way. The children are walkers of the same type; specifically, they have not yet left the domain A. Any walker starting in A may, as its first passage out of A, cross an outer boundary, in which case it terminates.

Consider now a walker whose first passage out of A is on the diagonal lm, as shown in Fig. 2. We turn it into

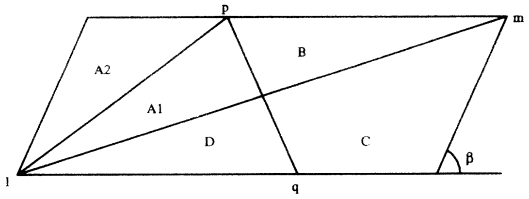

FIG. 1. A possible geometrical construction for a parallelogram, which is divided by the symmetry lines lm and pq into regions A,B,C,D. Region A is further divided into A1 and A2, respectively.

*Present address: CNLS, MS-B258, Los Alamos National Lab, Los Alamos, NM 87545.

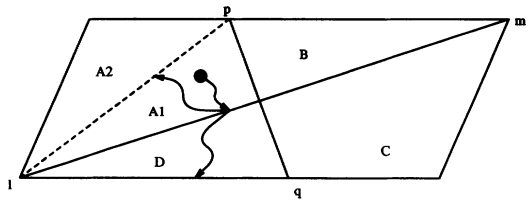

FIG. 2. A walker starting at region A1 crosses the symmetry line lm and splits into two walkers. One of them touches the outer boundary line lq later and vanishes while another continues in region A.

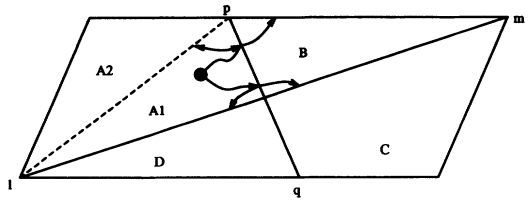

FIG. 4. Two scenarios for a walker whose first passage out of A is to cross the symmetry line pq. In one case, a walker in the region B touches the outer boundary and vanishes, while its partner continues in A. In another case, both walkers in the split pair next touch the diagonal line lm at inversion points and are terminated.

two walkers with weight one half each and which together follow correlated paths in which each is the reflection of the other in lm. The diagram shown in Fig. 2 displays one such pair one of whose members first touches an outer boundary; its partner touches the dashed line at the same time. The first terminates; the second continues its walk and possible branching in region A.

We now consider a walker that first crosses the diagonal and turns into a correlated pair, but whose next passage (out of A and D, respectively) crosses line pq, as illustrated in Fig. 3. Each of these points is an inversion of the other. An additional reflection of one walker in pq guarantees that all future points (dotted paths) retain that inversion symmetry. Such pairs will always give zero for any test function that has inversion symmetry. Therefore the pair need not be followed after the second crossing.

Figure 4 shows what happens when the first passage out of A crosses the line pq. In one outcome, a walker next touches the outer boundary and vanishes, having its partner to continue the walk (and branching) in A. Another pair is shown touching the diagonal at inversion points and terminating together.

The global outcome is that walkers move through regions A, B, and D but never enter C. Thus all walkers, including their partners, have overlaps with inversion antisymmetric test functions whose average value is bounded away from zero as the walks continue.

All walks are subject to branching determined by a trial eigenvalue. Unpaired walkers (which live in A only) may create other such walkers. Pairs symmetric in some line may create other such pairs whose future history follows the same rules independently.

Zhang and Kalos [4] have stressed the importance of the symmetry of positive and negative walkers in the fermion Monte Carlo method. In the present paper, there are no negative walkers. Nevertheless, the issue is essentially the same: for a particle in a box, walkers following ordinary dynamics will eventually distribute themselves symmetrically so that the average of any antisymmetric test function will be zero. The correlated walkers used here prevent this version of the fermion catastrophe.

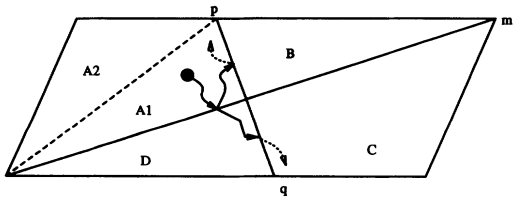

FIG. 3. A walker starting at region A1 first crosses the symmetry line lm and splits into two walkers. Both of them touch another symmetry line pq later and become two pairs with inversion symmetry. These pairs are terminated.

There is an alternative version of our method that uses walkers of both signs. In this point of view, walkers that make their first passage out of region A are also split into two, but one of the pair is reflected in the origin and given a negative sign. In two dimensions, this pair of walkers is then constrained to move so that their walks are mirror images in the line perpendicular to the one on which they were split. They are then guaranteed to meet at next passage on the mirroring line, and annihilate. The global outcome is that positive walkers can traverse regions A, B, and D, while negative walkers permeate regions B, C, and D. Here the plus-minus symmetry is broken and asymptotic overlaps with antisymmetric test functions are not zero.

II. A PARTICLE IN A TWO-DIMENSIONAL BOX WITH DIFFUSION MONTE CARLO

The first model we consider is a free particle confined in a rectangular box. The box is centered at the origin and has dimensions $2a \times 2b$ ($a \geq b > 0$). Our goal is to find the first excited state by the method described above. The analytical solution is of course trivially obtained and the nodal surface is simply $x = 0$. But, as mentioned in Sec. I, we will not make use of such knowledge.

The Schrödinger equation $\hat{H}\psi = E\psi$ written in the appropriate units is

$$-\nabla_R^2 \psi(R) = E\psi(R), \tag{1}$$

where $R = (x, y)$ is the coordinates of the particle and the solution $\psi(R)$ vanishes at the boundary of the box, i.e., $x = \pm a$ or $y = \pm b$. The corresponding eigenvalue is E. We will solve for the first antisymmetric wave function (under reflection at the origin) ψ_1 by a correlated random walk, using the antithetic pairing scheme imple-

mented with the diffusion Monte Carlo (DMC) method [1], a special case of the Green's function Monte Carlo method.

Define an operator g: $g(R,R') \equiv \langle R|\exp(-\tau\hat{H})|R'\rangle$, where τ is a positive constant. The DMC method is based on the idea that ψ_1 can be obtained from an arbitrary initial state $\psi^{(0)}$ by repetitively applying g, provided that $\psi^{(0)}$ has an antisymmetric component not orthogonal with ψ_1. In other words, with λ_T a trial eigenvalue, the equation

$$\psi^{(n)}(R) = \lambda_T \int g(R,R')\ \psi^{(n-1)}(R')\ dR', \tag{2}$$

will in principle lead to $\psi^{(\infty)} = \psi_1$.

The iterative procedure defined by Eq. (2) can be carried out as a random walk by Monte Carlo. In fact, in most cases it is the only possible way because the integral in Eq. (2) is in many dimensions. The wave function at each stage, $\psi^{(n)}$, is represented by an ensemble of discrete points (random walkers) $\{R\}^{(n)}$. In each iteration, walkers are advanced and multiplied by the kernel g to obtain new walkers for the next generation. The trial eigenvalue λ_T, when chosen properly, maintains on the average a constant population size in the random walk.

For the form of $\hat{H}$ in this problem, an approximation for g at small τ can be derived from the free diffusion operator by taking into account the boundary condition. That is, for $\tau \ll b^2$, the walkers can be treated as free Brownian particles until they are in the vicinity of the boundary of the rectangle. The kernel of the Brownian motion can be written as a product of Gaussians in both directions, each with variance 2τ. Explicitly,

$$g_0(R,R') = \frac{1}{4\pi\tau}\exp\Big[-\frac{(x-x')^2+(y-y')^2}{4\tau}\Big]. \tag{3}$$

To move R' by a step according to g_0 simply means sampling a pair of coordinates from the two-dimensional Gaussian centered at the old position. Inside the rectangle, the kernel g is well approximated by the free kernel g_0 in (3). Close to an absorbing boundary line, however, g must vanish as the line is approached. The correct form that ensures this can be obtained from the difference between the original free kernel at R' and the free kernel centered at its mirror image, i.e.,

$$\tilde{g}_0(R,R') = g_0(R,R') - g_0(R,PR'), \tag{4}$$

where P stands for the reflection with respect to the line. To advance a walker at R' according to $\tilde{g}_0$ in (4) implies sampling the Gaussian $g_0(R,R')$ and then accepting R with probability

$$p(R,R') \equiv 1 - \exp(-dd'/\tau), \tag{5}$$

where d and d' are the distances of the new and old positions from the line, respectively. The distance d is assigned a negative sign if the new position R is outside the boundary line; thus, a move to the outside of the absorbing boundary is never accepted, as should be the case. At the corners of the rectangle, mirror images generated by both sides are included and the kernel is

$$g_0(R,R') - g_0(R,P_aR') - g_0(R,P_bR') + g_0(R,P_aP_bR'), \tag{6}$$

where P_a and P_b denote reflections with respect to the two sides which form the corner. The expression above can also be written as a product of the two factors after modification by the image construction.

The simple random walk as outlined above will necessarily fail to generate the desired antisymmetric state, due to the fermion "sign" problem. That is to say, without explicit usage of the knowledge of the nodal surface at $x = 0$, the standard way of carrying out noninteracting random walks yields asymptotically a zero overlap with any antisymmetric test function. We shall show that, by incorporating into the random walk process the correlated pairs method as described in Sec. I, a stable antisymmetric component is ensured asymptotically and the "sign" problem is completely removed in this case. Other than technical issues related to the DMC implementation, the basic approach of correlated random walks discussed in Sec. I is directly applicable to the current problem. Random walkers diffuse according to the kernel g, with a typical step size controlled by the parameter τ. Since the random walks described by g are discrete with finite step sizes that are random at the symmetry lines, the probability of a walker landing precisely on the lines is zero. Thus, the details of first passage and crossing in general need to be addressed for the particular case here.

The symmetry lines are given by $y = kx$ and $y = -x/k$, where the slope k must satisfy $b/a \le k \le a/b$. Walkers are started in region A in the box, where $kx < y < -x/k$. When an initial walker first crosses a symmetry line, it is reflected with respect to that line and turned into a pair of correlated walkers, with the weight factor reduced by half. In these calculations, no weight factors are carried. So when a weight w is involved, a walker or pair is turned into int$[w+\xi]$ walkers or pairs, where ξ is a random number on $(0,1)$. Because of the finite step sizes, however, this "splitting" is done only after the first passage has occurred and the walker is already in either of the neighboring regions of A. This would introduce a discontinuity at the line, in precisely the same way as treating an absorbing boundary line by simply rejecting all walkers that cross it. To correct for this, the image construction is again used. With a finite probability, a walker that remains in A after a step but is within a small distance of a symmetry line is also reflected and turned into a pair. The probability is easily obtained from (5) and is given by $\exp(-dd'/\tau)$, where again d and d' are the distances from R and R' to the symmetry line.

Once an antithetic pair is formed, they remain mirror images and their random walks are always correlated, until one or both are absorbed. The former can happen if the image walker in region B or D is close to the boundary line, and the latter when the pair approaches the perpendicular symmetry line. In order to make the absorption smooth, we can again use the by now familiar image construction. In the first case, as the walker in B (or D) moves toward the boundary (and its partner

approaching the dashed line in Fig. 3), the pair remains a pair with probability p as given by (5). Otherwise it is reduced to an unpaired walker in A, with the image walker in B (or D) deleted. The probability p becomes 0 as the image walker reaches the boundary, as expected. Similarly, in the second case, the pair is removed from the population with probability $1-p$ as the walkers approach the perpendicular symmetry line.

At various corners, when more than one image is needed, the product of these kernels is used. When the angle at the corner is not $\pi/2$, however, this is only an approximation. The parameter τ is chosen small enough such that the error is negligible in our calculations.

This method of correlated walks clearly ensures a stable asymptotic antisymmetric component. The energy eigenvalue is given by

$$E = \frac{\sum_i \hat{H}\psi_T(R_i)}{\sum_i \psi_T(R_i)}, \tag{7}$$

where ψ_T is an antisymmetric trial wave function and the sum runs over all the walkers generated by the random walk after the initial relaxation phase. In these calculations a rather crude trial wave function was used: $\psi_T(R) = x(x^2 - a^2)(y^2 - b^2)$. We note that the method works correctly regardless of the specific choice of the symmetry lines, as long as they satisfy the prescription given in Sec. I. This is confirmed by our calculations.

For a square with side 2 ($a = b = 1$), the two symmetry lines are the diagonal lines. Our computed result is $E = 12.336 \pm 0.003$, in good agreement with the exact result of $E = 12.337$. For a rectangle with $a = 2$ and $b = 1$, we tested several values for the slope k of the symmetry line, all with satisfactory results. With $k = 0.9$, we obtained a first excited state energy of 4.936 ± 0.003, while the exact result is 4.9348.

In the case of a square, it is straightforward to see how the algorithm gives the correct solution. After relaxation, each walker in the population will have crossed one of the two symmetry lines and will therefore have become a pair. The population is naturally divided into two equal parts, each consisting of pairs that were created by the same symmetry line. These pairs are now confined in the region formed by the other symmetry line and two sides of the square. Thus asymptotically they represent a fixed-node solution with the other symmetry line as the node. The other half of the population behaves in a similar fashion. These two solutions, with the two diagonal lines as nodes, respectively, are both correct first excited state solutions and they add up to give the desired solution. For rectangles and even more general situations, a similar "decomposition" would include more complicated structures, but the possibility of obtaining the antisymmetric solution from the combination of several solutions analagous in some sense to those derived from a fixed-node method remains an intriguing one.

III. DOMAIN GREEN'S FUNCTION MONTE CARLO

In this section, we further explore the correlated pair algorithm discussed in Sec. I by utilizing a more sophisticated GFMC scheme to study the first excited state of the Schrödinger equation for a free particle moving inside an arbitrary parallelogram with hard walls. The wave function for the first excited state has inversion antisymmetry, namely, $\psi(R) = \psi(-R)$.

By introducing a Green's function $G(R, R')$, the Schrödinger equation can be written as

$$\psi(R) = E \int G(R, R')\psi(R')dR', \tag{8}$$

where E is the eigenvalue and $G(R, R')$ is defined as satisfying the following equation

$$\hat{H}G(R, R') = \delta(R - R'), \tag{9}$$

and $\hat{H}$ is the Hamiltonian of the system. The GFMC method is an exact algorithm that gives an iterative procedure whose asymptotic limit gives the state with the lowest E in Eq. (8).

In general, the Green's function for a many-body particle system is not known explicitly. Even for our simple model problem, the Green's function for the Schrödinger equation is not available analytically. One solution for this problem is to use some approximate schemes, such as the "short time" approximation for the Green's function used in the previous section. The so called domain GFMC (dGFMC) method to be used in this section is in principle, an exact scheme that samples the Green's function with the aid of the Monte Carlo technique. It samples a series of paths using a known Green's function in a small domain, usually one with some special geometry.

Assume we want to obtain the Green's function in the desired domain D of coordinate space. The first step is to find the solution of the Green's function in a subdomain $D_u(R_0)$ that is wholly contained within D with R_0 in $D_u(R_0)$. The subdomain Green's function is the solution of

$$\hat{H}G_u(R_1, R_0) = -\nabla_1^2 G_u(R_1, R_0) = \delta(R_1 - R_0), \tag{10}$$

which satisfies $G_u(R_1, R_0) = 0$ when R_1 is on the boundary of $D_u(R_0)$. With the help of Green's theorem, one can readily find that

$$G(R_1, R_0) = G_u(R_1, R_0) + \int_S [-\nabla_n G_u(R, R_0)]G(R_1, R)dR, \tag{11}$$

where S is the boundary of $D_u(R_0)$ and ∇_n is the outward-directed normal derivative with respect to R on S. Note that the integrand is positive because $G_u(R, R_0)$ is positive on $D_u(R_0)$ and zero outside. With the above expression, we are ready to sample $G(R_1, R_0)$ provided $G_u(R_1, R_0)$ is known. The details of how we sample $G(R_1, R_0)$ for our model problem are given in the Appendix A. More information related to this method can be found in Ref. [7].

The dGFMC paths are illustrated in Fig. 5. A walker is started from position 1 in the subregion A1. A rectangu-

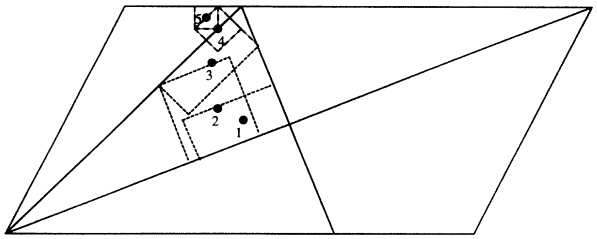

FIG. 5. An example of domain Green's function Monte Carlo paths. The walker starts at position 1 and continues until it touches the outer boundary, which is also the domain boundary for position 5.

lar domain is constructed centering around the position 1 within A1. The walker branches inside the rectangular box governed by the known Green's function G_u; the next position 2 is sampled on the boundary of the rectangular box according to the second term of Eq. (11). A rectangular domain centering around the position 2 is then constructed to repeat the same procedure. This process continues until the walker touches the hard-wall boundary of the parallelogram, which is also one boundary of the subdomain centered around the position 5. This gives one of the scenarios in which a walker terminates; others are explained in the previous sections when a second passage across the symmetry lines lm and pq happens. It also should be mentioned that walkers will not go forever even if they do not touch the symmetry lines, because a particle confined in a subregion has a larger eigenvalue than that if it moves inside the whole parallelogram. One advantage of this method compared to the "short time" approximation of the previous section is that we can identify precisely the event when the walker crosses a symmetry line.

The "minus sign" problem is circumvented by the correlated-pair scheme as discussed in the previous two sections. The Monte Carlo representation of the solution of the Schrödinger equation for the lowest antisymmetric state is given by

$$\psi_{1,MC}(R) = \sum_i [\delta(R - R_i) - \delta(R + R_i)], \tag{12}$$

where R_i represents the positions of the walkers found in the random walk after equilibration.

The code is first tested on a rectangular of length $2a = 4$ and width $2b = 2$. The first excited state energy obtained by our method is 4.9348(5), while the exact value is 4.9348. The following trial function was used in the mixed estimate:

$$\psi_T(R) = x(b^2 - y^2)(y^2 - 5b^2)(a^2 - x^2)(3x^2 - 7a^2). \tag{13}$$

The trial wave function has a correct nodal line $x = 0$, but our walkers cross it.

We proceeded to study a parallelogram, as shown in Fig. 1, with length $2a = 3$ and width $2b = 2$ and an angle of $\beta = 70°$. The trial wave function used has the following form

$$\psi_T(R) = x(b^2 - y^2)[y\cos\beta - (x + a)\sin\beta][y\cos\beta - (x - a)\sin\beta], \tag{14}$$

which satisfies the condition that it vanish on the four boundary lines of the parallelogram. The nodal line of the trial function is now different from the nodal line of the exact solution. The first excited state energy obtained is 7.029(2). The larger error bars of the eigenvalue for the parallelogram compared with the case of the rectangular is mainly due to the quality of the trial wave function. In Fig. 6, we show a contour plot of the wave function obtained by our dGFMC method. The contours join points on the surface that have the same value of height, with the left half side having a negative height. The nodal line clearly deviates from $x = 0$. Our algorithm works very well for the parallelogram.

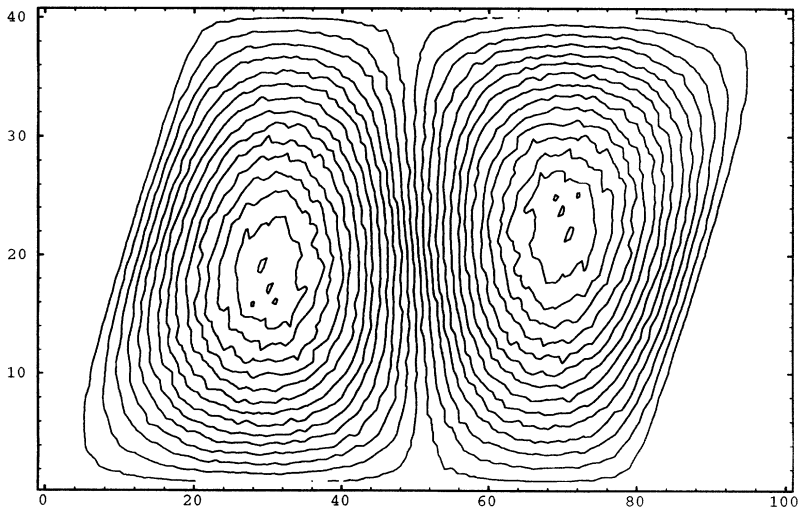

FIG. 6. The contour plot for the wave function of the first excited state in a parallelogram that has an inclined angle 70°. The rectangular frame is for the scale reference only.

IV. A GAUSSIAN MODEL IN TWO DIMENSIONS

The model used here [5] derives from the homogeneous integral equation in one dimension:

$$\psi_k(x) = \lambda_k \int \frac{1}{\sqrt{\pi}} e^{-(x-x')^2} \sqrt{2} e^{-\frac{1}{2}x'^2} \psi_k(x')dx'$$
$$= \lambda_k \int g_m(x,x')w(x')\psi_k(x')dx'; \quad (15)$$
$$g_m(x,x') = \frac{1}{\sqrt{\pi}} e^{-(x-x')^2},$$
$$w(x) = \sqrt{2} e^{-\frac{1}{2}x^2}.$$

Solutions exist for the eigenvalues $\lambda_k = 2^k$, $k = 0, 1, 2, \ldots$,

$$\psi_k(x) = p_k(x) e^{-x^2/2},$$

where p_k is a polynomial of order k. For the first four states, we have

$$p_0(x) = 1; \quad p_1(x) = x; \quad p_2(x) = x^2 - \frac{1}{3}; \quad p_3(x) = x^3 - x.$$

The general solution can be expressed as

$$p_k(x) = \sum_{n=0}^{\mathcal{M}} (a_{k,k-2n} x^{k-2n});$$

where $n = 0, 1, 2, \ldots, \mathcal{M}$, with $\mathcal{M} = \text{int}[k/2]$. If we choose $a_{k,k}$ as the normalization constant, the rest of the coefficients ($n > 0$ terms) can be derived from the following recursive relation:

$$a_{k,k-2n} = \frac{4^n}{1-4^n} \sum_{l=1}^{n} C^{2l}_{k-2n+2l} \frac{(2l-1)!!}{4^l} a_{k,k-2n+2l},$$

where $C^{2l}_{k-2n+2l}$ are binomial coefficients. More concisely, the polynomial p_k can also be obtained from

$$p_{k+1} = -\frac{1}{3} e^{3x^2/2} \frac{d}{dx} \left[e^{-3x^2/2} p_k(x) \right], \quad (16)$$

in which we choose $a_{k,k} \equiv 1$.

This model has some resemblance to a path integral for a harmonic potential. Its interest here lies in its simple random walk implementation: a walker at position x' branches so that, on the average, $\lambda_k w(x')$ walkers continue, and each such walker moves to position x, drawn at random from the probability density function $g_m(x,x')$. If a population of such walkers is iterated for many steps, the asymptotic density is $\exp(-x^2/2) = \psi_0(x)$, and using the factor λ_k makes the population asymptotically constant, on the average.

The expression

$$\lambda = \frac{\int \psi_T(x) w(x) \psi_T(x) dx}{\int\int \psi_T(x) w(x) g_m(x,x') w(x') \psi_T(x') dx dx'} \quad (17)$$

is a variational upper bound for the lowest eigenvalue, given the correct symmetry. The function ψ_T is a trial wave function not orthogonal to ψ_0. Based upon this, we expect that a "mixed estimator" would be effective that uses a good trial function as well as the Monte Carlo information about the solution:

$$\psi_{\text{MC}}(x) = \sum_j \delta(x - x_j). \quad (18)$$

In the last expression, x_j is the set of positions at which walkers are found after equilibration. Such a mixed estimator is

$$\lambda = \frac{\int \psi_T(x) w(x) \psi_{\text{MC}}(x) dx}{\int\int \psi_T(x) w(x) g_m(x,x') w(x') \psi_{\text{MC}}(x') dx dx'}$$
$$= \frac{\sum_j \psi_T(x_j) w(x_j)}{\sum_j \int \psi_T(x) w(x) g_m(x,x_j) w(x_j) dx}. \quad (19)$$

As discussed in the Ref. [5], the importance sampling transformation for this model problem has the form

$$\tilde{\psi}_k(x) = \psi_0(x) w(x) \psi_k(x)$$
$$= \lambda_k \int [\psi_0(x) w(x) g_m(x,x') / \psi_0(x')] \tilde{\psi}_k(x') dx'$$
$$= \lambda_k \int \tilde{g}_m(x,x') \tilde{\psi}_k(x') dx'; \quad (20)$$
$$\tilde{g}_m(x,x') = \sqrt{\frac{2}{\pi}} \exp[-2(x - x'/2)^2]. \quad (21)$$

For $k = 0$, $\lambda_k = 1$, and the kernel is normalized to unity. Implementation of the random walk that derives from the importance sampled equation requires no branching, and involves a rescaling of the previous coordinate, $x' \to x'/2$ to get the centroid of the Gaussian from which the next position is sampled.

When using this form of the equations and of the random walks, our estimate of the solution for $\tilde{\psi}_{\text{MC}}(x)$ is again given by a sum of δ functions similar to Eq. (18). Thus, the corresponding mixed estimator for the eigenvalue is

$$\lambda = \frac{\sum_j \psi_T(x_j)/\psi_0(x_j)}{\sum_j \int \psi_T(x)/\psi_0(x) \tilde{g}_m(x,x_j) dx}. \quad (22)$$

Solutions for the multidimensional Gaussian model can be built up from solutions in one dimension. For example, in the case of two dimensions,

$$\psi_{k,l}(R) = \psi_k(x)\psi_l(y) \quad (23)$$

has eigenvalue $\lambda_k \lambda_l$. In the present work, we seek a solution to our Gaussian Model in two dimensions that vanishes on $y = -x$ and that is antisymmetric on inversion in the origin. In applying our method of perpendicular lines, we introduce two lines $x = 0$ and $y = 0$ to define geometric domains. Walkers are introduced in the first quadrant only (in fact along the line $x = y$). Following our construction these walkers move according to the rules for the Gaussian model, modified by importance sampling for the ground state. That is, a walker at R_0 moves to $R_0/2$ and then to a differenct point sampled

from a Gaussian $\tilde{g}(R, R_0) = \frac{2}{\pi} \exp[-2(R - R_0/2)^2]$ centered about the rescaled position. Clearly walkers are conserved. Let us leave aside the question of how to define "first passage" across a surface for a model that alternates coordinate rescalings and discrete steps sampled from a Gaussian. Otherwise, the construction goes as before: Upon first passage at either $y = 0$ or $x = 0$, a walker splits into walkers (of weight one half each) which then move as mirror images reflected in the line just touched, until they both touch the other coordinate line. At that stage the walkers are at points that image each other by inversion in the origin and their walk is terminated.

First passage events are defined as follows. Consider a walker at R_0. After the rescaling required by the importance sampled kernel, it is moved to $R_0/2$, a move that does not cross either coordinate line. The next step is to sample R from a Gaussian kernel $\tilde{g}(R, R_0)$. This kernel can be thought of as a Green's function of the heat equation in two dimension

$$g_t(R, R_0, t) = \frac{1}{4\pi t} \exp\left(-\frac{(R - R_0/2)^2}{4t}\right); \quad t = \frac{1}{8}.$$

We may follow walkers through a process that simulates the Brownian motion from $R_0/2$ up to time $t = \frac{1}{8}$ either by approximating a Brownian path or by using exact Green's functions. We only discuss the latter here. A source at point R_s above a line satisfies the recurrence

$$g_t(R, R_s, t) = \int_0^t \int_{-\infty}^{\infty} g_t(R, R', t - t') \times \left[-\frac{\partial g_0(R', R_s, t')}{\partial n}\right] dR' dt', \tag{24}$$

where $\frac{\partial g_0(R', R_s, t')}{\partial n}$ is the outer normal derivative of the Green's function for the heat equation that vanishes on the line. The latter is obtained from an image construction and is

$$g_0(R, R_s, t) = \frac{1}{4\pi t}\Big[\exp[-(R - R_s)^2/4t] - \exp[-(R - R_I)^2/4t]\Big], \tag{25}$$

where R_I is the image of R_s in the line. If the line is $y = 0$ and $R_s = (0, y_s), R_I = (0, -y_s)$, then

$$g_0(R, R_s, t) = \frac{1}{4\pi t} \exp\left(-\frac{x^2 + (y - y_s)^2}{4t}\right) \times \left[1 - \exp\left(-\frac{y y_s}{t}\right)\right],$$

$$-\frac{\partial g_0(R, R_s, t)}{\partial n} = \frac{\partial g_0(R, R_s, t)}{\partial y}\Big|_{y=0} = \frac{y_s}{4\pi t^2} \exp\left(-\frac{x^2 + y_s^2}{4t}\right). \tag{26}$$

The last expression is a joint probability distribution for a position x and time t for a first passage across the line in question. The marginal distribution for x is obtained by integrating in t:

$$m(R|R_s) = \int_0^{\infty} \left[-\frac{\partial g_0(R, R_s, t)}{\partial n}\right] dt = \frac{y_s}{\pi(x^2 + y_s^2)}, \tag{27}$$

which may be sampled as

$$x = y_s \tan[\pi(\xi - \tfrac{1}{2})]. \tag{28}$$

Given a value of x as chosen, a value of t sampled jointly with that x from Eq. (26) is

$$t = \frac{x^2 + y_s^2}{-4 \ln \xi}, \tag{29}$$

where ξ is a uniform random number between 0 and 1.

Note that this applies directly to the first passage crossing of either member of a correlated pair. The first stage crossing is out of quadrant A, where either $y = 0$ for $x > 0$ or $x = 0$ for $y > 0$ is crossed. We proceed as above constructing a Green's function that vanishes on both these lines; three images are needed. Rejection methods for sampling coordinates and times are easily set up. Note also that after a crossing at time t' there remains $t - t' = 1/8 - t'$ left for the path in question. A next event is sampled from a Green's function in an appropriate region (or from next passage across another line) using the appropriate time remaining.

A program was written embodying these ideas and algorithms. The test function was taken to be

$$\psi_T(R) = \exp[-(R - R_T)^2] - \exp[-(R + R_T)^2], \tag{30}$$

with $R_T = (6^{-1/2}, 6^{-1/2})$. To keep the program simple,

TABLE I. Eigenvalues computed for the lowest antisymmetric state of the Gaussian model in two dimensions with different fixed population sizes N. In addition to the value of N, the computed eigenvalue and its standard error, we show an estimate of the population bias, and its standard error.

N	Eigenvalue	Standard error	N^* (eigenvalue -2)	N^* standard error
2500	2.00003729	0.00000450	0.0932	0.0113
5000	2.00001830	0.00000385	0.0915	0.0193
10000	2.00000600	0.00000325	0.0600	0.0325

the population of walkers was fixed in a naive way. It was necessary, therefore to run at several populations and extrapolate the eigenvalue to infinite population. A number of completely independent runs were made at populations fixed at 2500, 5000, and 10 000 walkers. The results are shown in Table I. The fourth column shows the eigenvalue bias times the population size; it is constant within the appropriately reduced errors (column five). That is, the results are consistent with a bias proportional, within this range, to $1/N$. Hence a weighted least square fit to a straight line in $1/N$ was made. The result is an eigenvalue extrapolated to $1/N = 0$ of 1.999 996 24, with an estimated standard error of 0.000 004 32. This agrees with the correct eigenvalue, namely, 2.

Two-dimensional histograms are also in agreement with those derived from the exact eigenfunctions, when two of the latter are combined, one with x=0 as node, the other with y=0.

V. DISCUSSION

We note that the boundaries in the problem can be perturbed in various ways without invalidating the construction discussed in Sec. I. Obviously the geometry must always satisfy inversion symmetry. Given that, the key to the method is to establish the "base" region (A in Fig. 1) and prevent walkers from entering its inversion region (C). For the algorithm to succeed in this form, the neighboring regions (B and D) must be completely contained in the "base" region upon reflection at the symmetry lines. This ensures that all walkers in the neighboring regions are paired, each with an antithetic walker in the "base" region. Any entry of such a paired walker to the "prohibited" region C leads to a symmetric pair at inversion, which can then be eliminated; thus the entry is indeed prohibited. With this satisfied, details of the geometry do not affect the success of the algorithm. That is, the boundaries can be arbitrary provided that, under some choice of symmetry lines, all neighboring regions fall within the base region after reflection. The geometry shown in Fig. 7 is one such example.

We also mention that the method remains applicable even in the presence of certain forms of potentials with inversion symmetry in addition to or instead of hard wells. Recall that the potential $V(R')$ affects the multiplicity of a walker at R' in the random walk process. In the DMC method, at the small τ limit the potential appears in the random walk directly as a weight factor, $\exp(-\tau V(R'))$.

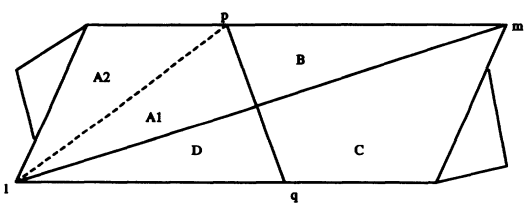

FIG. 7. Geometries can be constructed by perturbing the boundaries of the parallelogram without invalidating our method.

In the dGFMC method, it manifests itself as the continuation probability for the random walk with which the Green's function $G(R, R')$ is sampled, $1 - V(R')/U$, where U is a constant chosen such that $U \geq V(R')$. We see that in either case, the larger the potential $V(R')$ is, the smaller the multiplicity becomes for a walker at R'. Therefore, if the potential at any position in the neighboring region B or D is no less than the value at the reflected point in the "base" region A, it can be arranged that a walker in B or D always remains a member of a pair. It is then guaranteed that walkers will never enter region C and the algorithm will work successfully. This provides yet another simple illustration of the general principle discussed in the previous paragraph.

Finally, the method is by no means limited to two dimensions. The basic principle outlined in Sec. I can be easily generalized to higher dimensions. For example, for a d-dimensional hypercube centered at the origin, we can construct all the symmetry surfaces as $(d-1)$-dimensional hyperplanes, with each containing $d-1$ axes. A walker denoted by $(x_1, x_2, x_3, \ldots, x_d)$ is followed until it touches a symmetry plane, that is, one of the coordinates, say x_k, becomes zero. We then split the walker into a correlated pair of walkers with each carrying a weight of one half. The coordinate of the mirror image walker is given by $(x_1, x_2, x_3, \ldots, -x_k, \ldots, x_d)$. The pair is followed until another coordinate, say x_j, of both walkers is on its corresponding symmetry plane. The walkers are not split this time. Instead, the coordinates of the image walker become $(x_1, x_2, x_3, \ldots, -x_k, \ldots, -x_j, \ldots, x_d)$. This procedure continues as successive coordinates are reflected. The walk stops when the last symmetry plane is reached, i.e., the last coordinate is reflected.

ACKNOWLEDGMENTS

We are happy to thank David Ceperley and Geoffrey Chester for helpful conversations, and particularly Cyrus Umrigar for a most insightful comment. This work was supported in part by the National Science Foundation (NSF) under Grant No. DMR-9200469. The Cornell Theory Center is funded by the NSF, by New York State, by IBM, and by Cornell University.

APPENDIX: SAMPLING DOMAIN GREEN'S FUNCTION

Let us consider the case where the subdomain $D_u(R_0)$ is a rectangle. It is clear that $D_u(R_0)$ is a Cartesian product of two one-dimensional subspaces, $D_u(R_0) = d_x(x_0) \otimes d_y(y_0)$. Define $g(x, x_0, t)$ that satisfies

$$-\frac{\partial^2}{\partial x^2} g(x, x_0, t) + \frac{\partial}{\partial t} g(x, x_0, t) = 0, \qquad \text{(A1)}$$
$$g(x, x_0, 0) = \delta(x - x_0),$$

and $g(x, x_0, t) = 0$ on the boundary of $d_x(x_0)$ and outside of $d_x(x_0)$. The same equation holds for the y direction; $g(y, y_0, t)$ vanishes on $d_y(y_0)$ and outside $d_y(y_0)$. Thus

for R, R_0 in D_u, it is easy to show that the function

$$G_u(R, R_0) = \int_0^\infty g(x, x_0, t) g(y, y_0, t) dt \tag{A2}$$

is the Green's function that satisfies the definition (10). The Eq. (A1) can be solved analytically. For $-a_1 \leq x, x_0 \leq a_1$, the solution is

$$g(x, x_0, t) = \frac{1}{a_1} \sum_{k=1}^{\infty} \sin\left(\frac{k\pi}{2a_1}(x + a_1)\right) \times \sin\left(\frac{k\pi}{2a_1}(x_0 + a_1)\right) \exp\left[-\left(\frac{k\pi}{2a_1}\right)^2 t\right]. \tag{A3}$$

With a known expression of $g(R, R_0, t)$, sampling $G(R_1, R_0)$ of Eq. (11) becomes an issue of how to sample $G_u(R_1, R_0)$ and the normal derivative $-\nabla_n G_u(R, R_0)$ for $R \in S$. In order to sample $G_u(R, R_0)$, we rewrite Eq. (A2) as

$$G_u(R, R_0) = \int_0^\infty u \exp(-ut) \left[\frac{g(x, x_0, t)}{H_x(t)} \frac{g(y, y_0, t)}{H_y(t)}\right] \times H_x(t) H_y(t) \frac{\exp(ut)}{u} dt, \tag{A4}$$

$$H_x(t) = \int_{-a+x_0}^{a+x_0} g(x, x_0, t) dx, \tag{A5}$$

in which $H_x(t)$ satisfies $H_x(0) = 1$ and $H_x(\infty) = 0$, and u is an arbitrary positive parameter. It is best to choose u such that the t dependence of $\exp(-ut)$ is close to the distribution to be sampled. In our calculation, u is chosen as $(\pi/2a_1)^2 + (\pi/2a_2)^2$, with a_1 and a_2 being the length and width of the rectangular domain. We first sample t from $u\exp(-ut)$. Using this value, we proceed to sample x, y from x_0, y_0 using the kernel given in the bracket in the above equation. The product of the trial eigenvalue and the factor $H_x(t)H_y(t)\exp(ut)/u$ is used as a factor to determine the multiplicity of branching of a walker moved from R_0 to R.

The sampling of the normal derivative term on the surface S is little more tricky. We find that the derivative of $H_x(t)$ with respect to t is

$$\begin{aligned} H_x'(t) &= \int_{-a+x_0}^{a+x_0} \frac{\partial}{\partial t} g(x, x_0, t) dx \\ &= \int_{-a+x_0}^{a+x_0} \frac{\partial^2}{\partial x^2} g(x, x_0, t) dx \\ &= \int_{S_x} \nabla_{nx} g(x, x_0, t) dx, \end{aligned} \tag{A6}$$

where S_x is the boundary of d_x and ∇_{nx} is the outward directed normal derivative with respect to x. Thus the derivative term of Eq. (11) becomes

$$\begin{aligned} -\nabla_n G_u(R, R_0) &= \int_0^\infty [-\nabla_{nx} g(x, x_0, t)] g(y, y_0, t) dt + \int_0^\infty [-\nabla_{ny} g(y, y_0, t)] g(x, x_0, t) dt \\ &= \int_0^\infty [-H_x'(t) H_y(t)] \left[\frac{\nabla_{nx} g(x, x_0, t)}{H_x'(t)}\right] \left[\frac{g(y, y_0, t)}{H_y(t)}\right] dt \\ &\quad + \int_0^\infty [-H_y'(t) H_x(t)] \left[\frac{\nabla_{ny} g(y, y_0, t)}{H_y'(t)}\right] \left[\frac{g(x, x_0, t)}{H_x(t)}\right] dt. \end{aligned} \tag{A7}$$

Suppose t_x and t_y are drawn independently from $H_x'(t)$ and $H_y'(t)$, respectively. The probability that the smaller one is t_x and that t_x lies in a small interval of time dt near t is $H_x'(t)dt[\int_t^\infty H_y'(t_y)dt_y] = -H_x'(t)H_y(t)dt$. Thus, we use the following method to sample the derivative term $-\nabla_n G_u(R, R_0)$. We first sample t_x and t_y from $H_x'(t)$ and $H_y'(t)$, respectively. If $t_x < t_y$, we sample R on $S_x \otimes d_y(y_0)$ using the kernel at t_x given by the brackets of the first integrand of Eq. (A7); otherwise, we use the kernel at t_y given by the second integrand of the same equation and sample R on $S_y \otimes d_x(x_0)$.

The process of sampling t from $H_x'(t)$ is accomplished by setting the corresponding cumulative distribution function equal to a uniform random number, namely, $1 - H_x(t) = \xi$. Thus, $t = H_x^{-1}(\xi')$, where $\xi' = 1 - \xi$. The inversion is implemented by matching ξ' with a precomputed table of $H_x(t)$.

An important question unanswered so far is how to sample the infinite series such as Eq. (A3). First, we notice that $g(x, x_0, t)$ is a function of three dimensionless variables, $\rho = x/a_1$, $\rho_0 = x_0/a_1$, and $\tau = t/a_1^2$. The advantage of this dimensionless form is that the function $ag(\rho, \rho_0, \tau)$ is independent of the particular size of the rectangular subdomain. In the case of large τ, then Eq. (A3) converges rapidly. For $\tau > 0.08$, we only need use the first five terms in the sum for sampling x to achieve accurate results. However, if τ is small, the eigenfunction expansion (A3) is only slowly converging and an alternative method of sampling $g(x, x_0, t)$ is necessary. We accomplish this by developing the short time expansion of $g(x, x_0, t)$. By using the Poisson sum rule

$$\sum_{n=-\infty}^{\infty} \exp[-(\rho - \rho_0 + 2n)^2/4\tau] = \sqrt{(\pi\tau)} \left[1 + 2\sum_{n=1}^{\infty} \cos[n\pi(\rho - \rho_0)] \exp[-(n\pi)^2\tau]\right]. \tag{A8}$$

we find that

$$ag(\rho, \rho_0, \tau) = \frac{1}{\sqrt{(4\pi\tau)}} \sum_{m=-1}^{m=1} (-1)^m \times \exp[-(\rho - \rho_0 + 2m)^2/4\tau] \tag{A9}$$

is a very good approximation for $\tau \leq 0.08$.

[1] J.B. Anderson, J. Chem. Phys. **63**, 1499 (1975); **65**, 4121 (1976); **73**, 3897 (1980). See, e.g., B.H. Wells, in *Methods of Computational Chemistry*, edited by S. Wilson (Wiley, New York, 1987), Vol. 1; K.E. Schmidt and M.H. Kalos, in *Applications of the Monte Carlo Method in Statistical Physics*, edited by K. Binder (Springer-Verlag, Berlin, 1984).

[2] D.M. Arnow, M.H. Kalos, Michael A. Lee, and K.E. Schmidt, J. Chem. Phys. **77**, 5562 (1982).

[3] J.B. Anderson, C.A. Traynor, and B.M. Boghosian, J. Chem. Phys. **95**, 7418 (1991).

[4] Shiwei Zhang and M.H. Kalos, Phys. Rev. Lett. **67**, 3074 (1991).

[5] M.H. Kalos, J. Stat. Phys. **63**, 1269 (1991).

[6] D.M. Ceperley and M.H. Kalos, in *Monte Carlo Methods in Statistical Physics*, edited by K. Binder (Springer-Verlag, Berlin, 1979).

[7] M.H. Kalos, D. Levesque, and L. Verlet, Phys. Rev. A **9**, 2178 (1974).

[8] M.H. Kalos, Phys. Rev. **128**, 1791 (1962).